Biotic Interactions and Plant Invasions in Subtropical Riparian Ecosystems: Experimental and Demographic Evidence from Hangzhou, China

Author: William Morris 1

1 Visiting Scholar, College of Life Sciences, Zhejiang University, Hangzhou 310058, China

Abstract

Biotic interactions—encompassing herbivory, pathogen infection, mutualistic pollination, and belowground microbial associations—govern the establishment, colonization, and persistence of non-native plant species. While the Enemy Release Hypothesis (ERH) posits that invasive taxa proliferate due to the absence of co-evolved specialist antagonists, the Biotic Resistance Hypothesis (BRH) suggests that native assemblages suppress exotic spread. Few empirical studies, however, integrate multiple antagonist and mutualist guilds within a unified demographic framework to quantify their net influence on population trajectory (λ).

This study investigates the multi-trophic biotic interactions regulating the invasive perennial *Solidago canadensis* L. in comparison with its co-occurring native congener *Solidago decurrens* Lour. across riparian and wetland fringes in Hangzhou, Zhejiang Province, China. Utilizing a multi-site, full-factorial field experiment (insect exclusion via systemic insecticide, soil-borne fungal pathogen suppression via fungicide drench, and pollinator exclusion) replicated across six riparian ecosystems in the Hangzhou urban-rural ecotone, we monitored vital rates over three consecutive growing seasons (2023–2025).

We embedded these empirical demographic rates into stage-structured matrix population models to estimate asymptotic population growth rates (λ) and elasticity values. Native *S. decurrens* suffered pronounced demographic penalties under ambient conditions due to severe root-associated fungal pathogen loads, depressing its projected growth rate ($\lambda = 0.934 \pm 0.038$). Conversely, *S. canadensis* demonstrated pronounced tolerance to generalist foliar insect herbivory and neutral plant-soil feedbacks under ambient microbiota, while simultaneously capitalizing on native generalist pollinators to secure substantial seed set. The projected population growth rate for *S. canadensis* remained well above unity across all treatments ($\lambda_{\text{ambient}} = 1.158 \pm 0.041$). Elasticity analyses revealed that the demographic persistence of *S. canadensis* is heavily cushioned by clonal ramet survival and vegetative transitions, rendering it resilient against local antagonistic pressures. Effective ecological suppression of *S. canadensis* in subtropical China necessitates integrated management strategies targeting clonal vegetative expansion alongside native plant-soil community restoration, rather than relying exclusively on single-guild biological controls.

Keywords: *Solidago canadensis*, Enemy Release Hypothesis, Biotic Resistance, Matrix Population Models, Subtropical Wetlands, Elasticity Analysis, Hangzhou.

1. Introduction

Biological invasions present severe ecological and economic threats to global biodiversity, transforming community structures, altering nutrient cycles, and destabilizing indigenous trophic networks (Elton, 1958; Van Kleunen et al., 2010). Among the fundamental mechanisms determining whether an introduced plant establishes viable, self-sustaining populations is the

balance of biotic interactions it encounters in the recipient community (Mitchell & Power, 2003; Levine et al., 2004).

Two foundational yet contrasting paradigms dominate the conceptual landscape of invasion biology:

1. **The Enemy Release Hypothesis (ERH):** Asserts that non-native species leave behind specialized natural enemies (herbivores, nematodes, and pathogens) from their native ranges, conferring a competitive advantage over co-occurring native competitors that remain burdened by their own specialized antagonists (Keane & Crawley, 2002; Maron & Vilà, 2001).

2. **The Biotic Resistance Hypothesis (BRH):** Posits that intact native recipient communities—through diverse guilds of generalist herbivores, competitors, and indigenous pathogens—effectively suppress prospective invaders and buffer against aggressive colonization (Elton, 1958; Levine et al., 2004).

Historically, empirical evaluations of these hypotheses have focused on individual interaction pathways in isolation, such as quantifying foliar herbivory rates or measuring seedling mortality induced by soil oomycetes (Bever et al., 2012; Callaway et al., 2004). However, plants in natural communities interact simultaneously with complex assemblages of mutualists (e.g., pollinators, mycorrhizal fungi) and antagonists (e.g., folivores, stem borers, seed predators, and root-rot pathogens) (Morris et al., 2007).

Crucially, measuring damage or visitation metrics alone fails to provide a conclusive forecast of invasion success. A 20% reduction in foliar tissue from generalist chewers may exert negligible influence on the population growth rate of a plant capable of compensatory photosynthesis or extensive clonal propagation, whereas a minor reduction in seedling recruitment or seed set could drive a non-clonal species toward local extinction (Caswell, 2001; Morris & Doak, 2002). Therefore, resolving the net ecological outcome of multiple simultaneous biotic interactions requires coupling experimental community manipulations with demographic matrix population models (Morris et al., 2007, 2008).

The Yangtze River Delta in eastern China, characterized by rapid urbanization, high-density waterway networks, and extensive agricultural-urban transition zones, represents an active epicenter of plant invasions (Ding et al., 2006). Hangzhou, the capital of Zhejiang Province ($30°15′\,\mathrm{N}, 120°10′\,\mathrm{E}$), possesses a subtropical monsoon climate characterized by hot, humid summers and mild winters, crossed by extensive riverine corridors, wetland reserves (such as Xixi National Wetland Park), and lacustrine systems.

Over the past three decades, *Solidago canadensis* L. (Canada goldenrod, Asteraceae), a rhizomatous perennial native to North America, has extensively invaded Hangzhou's riparian fringes, abandoned agricultural lands, and transport verges (Dong et al., 2015; Lu et al., 2013). In these habitats, *S. canadensis* frequently displaces the native congener *Solidago decurrens* Lour., forming monospecific stands that compromise native plant diversity and impair riparian ecological integrity.

While physiological and allelopathic characteristics of *S. canadensis* have been documented, the degree to which multi-trophic biotic interactions govern its demographic divergence from native congeners in eastern China remains unresolved. Specifically, we address three critical questions:

1. Does *S. canadensis* experience lower antagonist pressure (herbivores and fungal pathogens) and higher mutualist visitation (pollinators) compared to native *S. decurrens* in Hangzhou's riparian habitats?

2. How do individual vital rates (germination, vegetative survival, clonal growth, flowering probability, and fecundity) respond to the experimental exclusion of insect herbivores, soil pathogens, and pollinators?

3. When integrated into demographic projection models, how do these multi-guild biotic interactions alter the finite rate of population increase (λ), and which life-history transitions exhibit the highest elasticity for invasion control?

2. Materials and Methods

2.1 Study Site and Environmental Characterization

Field experiments were conducted across six distinct riparian and wetland reserve zones in Hangzhou, Zhejiang Province, China, spanning the Xihu, Yuhang, and Gongshu administrative districts:

- Site 1 & 2: Xixi National Wetland Park outer periphery ($30°16′12″\text{N}, 120°03′45″\text{E}$)
- Site 3 & 4: Liangzhu riparian reserve along the Tiaoxi River ($30°22′30″\text{N}, 119°59′18″\text{E}$)
- Site 5 & 6: Qiantang River riparian greenway corridor ($30°18′04″\text{N}, 120°20′52″\text{E}$)

The region experiences a mean annual temperature of $16.5°\text{C}$, with July monthly means reaching $28.6°\text{C}$ and January means hovering around $4.3°\text{C}$. Mean annual precipitation is approximately $1{,}450$ mm, with over 60% occurring during the East Asian rainy season (Meiyu period, May to August). Soils across all study plots are classified as alluvial hydromorphic soils characterized by sandy-loam to silt-loam textures, neutral-to-slightly-acidic pH ($6.2 - 6.8$), and high organic matter content ($2.4 - 3.8\%$).

2.2 Study Species

- *Solidago canadensis* L. is a clonal C3 perennial herb producing erect stems ($1.0 - 2.5$ m tall) from dense underground rhizome networks. It blooms from late August to October in Hangzhou, producing hundreds of small capitula grouped into pyramidal panicles pollinated by generalist insects, accompanied by wind-dispersed achenes.
- *Solidago decurrens* Lour. is a native perennial congener occurring in open fields and forest margins across central and southern China. It exhibits a smaller stature ($0.3 - 1.0$ m tall), weaker rhizomatous tillering, and smaller corymbose inflorescences flowering concurrently from September to November.

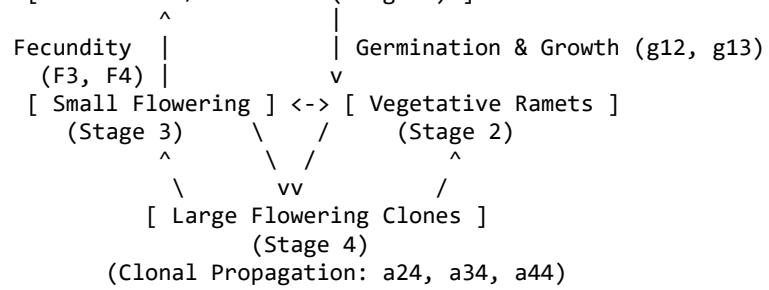

2.3 Factorial Experimental Design

To evaluate the isolated and synergistic contributions of biotic interactions, we implemented a $2 \times 2 \times 2$ factorial randomized complete block design replicated across the six field sites:

1. **Factor 1: Insect Herbivore Exclusion (H)**

   - *Exclusion (H^-):* Foliar spray of systemic insecticide (0.05% active ingredient imidacloprid combined with 0.02% esfenvalerate) applied bi-weekly from April to October.
   - *Control (H^+):* Equivalent volume foliar spray of ambient water.

2. **Factor 2: Soil-Borne Fungal Pathogen Suppression (F)**

   - *Suppression (F^-):* Soil drench using broad-spectrum systemic fungicides (metalaxyl-M at 0.5 g/L to suppress Oomycota, combined with carbendazim/benomyl at 1.0 g/L targeting Ascomycota and Basidiomycota) applied monthly within a 0.5-m radius of focal stems.
   - *Control (F^+):* Equivalent soil water drench.

3. **Factor 3: Pollinator Accessibility (P)**

   - *Exclusion (P^-):* Inflorescence branches bagged with fine, breathable micro-mesh (0.2 mm pore size) immediately prior to bud anthesis to exclude insect visits while allowing natural airflow.
   - *Open Pollination (P^+):* Unrestricted natural visitation by local flower-visiting insects.

At each of the 6 sites, 10 experimental blocks were established. Within each block, experimental subplots (2.0 m $\times$ 2.0 m) were assigned to each combination of treatments for both species ($N = 6$ sites $\times$ 10 blocks $\times$ 8 treatment combinations $= 480$ focal plots, monitoring a total of 1,920 marked individuals over 2023–2025).

2.4 Demographic Rate Measurements

Vital rates were recorded at discrete seasonal intervals across the three-year duration:

- **Vegetative Damage:** Evaluated in June and August by visually quantifying percentage foliar area removed or necrotic across 20 randomly selected leaves per stem. Root health was assessed on subset satellite harvest cores using root necrotic scoring ($0 - 5$ scale).
- **Survival (σ_i) and Transition Probabilities (g_{ij}):** Individual ramets were permanently marked with aluminum ring tags. Stems were classified annually into four discrete demographic stages:

1. *Stage 1 (Seedlings/New Recruits):* Stems < 15 cm in height emerging from seed.
2. *Stage 2 (Non-flowering Vegetative Ramets):* Stems > 15 cm lacking inflorescences.
3. *Stage 3 (Small Flowering Stems):* Reproductive stems < 80 cm in height.
4. *Stage 4 (Large Flowering Multi-stem Clones):* Reproductive clusters/stems ≥ 80 cm in height with secondary branching.

- **Reproductive Parameters (f_i, m_i):** Measured as the proportion of stems flowering (f_i), number of capitula per panicle, seed number per capitulum, and achene viability determined via 1% 2,3,5-triphenyltetrazolium chloride (TTC) assays.
- **Clonal Proliferation:** Number of newly sprouted rhizome daughter ramets recorded annually per square meter.

2.5 Matrix Population Modeling Framework

Following standard demographic formulations (Caswell, 2001; Morris et al., 2007), we constructed stage-classified Lefkovitch projection matrices (**A**) for each treatment combination and species:

$$\mathbf{n}_{t+1} = \mathbf{A}\mathbf{n}_t$$

Where:

- F_i represents sexual fecundity per individual in stage i, defined as $F_i = \sigma_i \times$ (flowering probability) $\times$ (viable seeds produced) $\times$ (seed-to-seedling emergence probability r).
- P_{ii} represents the probability of surviving and remaining in stage i.
- g_{ji} denotes the transition probability from stage i to a larger stage j.
- C_{ji} corresponds to clonal production of stage j ramets by stage 4 parental rhizomes.

The finite rate of population increase (λ) was computed as the dominant real eigenvalue of matrix **A**, satisfying:

$$\mathbf{A}\mathbf{w} = \lambda\mathbf{w}$$

Where $\mathbf{w}$ is the right eigenvector representing the stable stage distribution. The left eigenvector $\mathbf{v}$ satisfies $\mathbf{v}^T\mathbf{A} = \lambda\mathbf{v}^T$, representing the stage-specific reproductive values.

To isolate which demographic processes most strongly affect population growth across our biotic manipulation regimes, we calculated the matrix elasticity coefficients (e_{ij}), representing the proportional change in λ resulting from a proportional change in matrix element a_{ij}:

$$e_{ij} = \frac{a_{ij}}{\lambda}\frac{\partial\lambda}{\partial a_{ij}} = \frac{a_{ij}}{\lambda}\frac{v_i w_j}{\langle \mathbf{v}, \mathbf{w}\rangle}$$

Where $\sum_{i,j} e_{ij} = 1.0$ (Caswell, 2001; Morris & Doak, 2002). Standard errors and 95% confidence intervals for λ and e_{ij} were generated via 2,000 bootstrap iterations stratified across experimental blocks.

2.6 Statistical Analyses

We analyzed leaf damage percentages, seed production, and vital rates using Generalized Linear Mixed-Effects Models (GLMM). Foliar damage was modeled under a beta error distribution with a logit link function. Seed viability and survival probabilities were fitted with binomial logistic mixed models. Continuous performance metrics (biomass, stem heights) were evaluated using Linear Mixed-Effects Models (LMM) with Gaussian errors.

Fixed factors included Species (*S. canadensis* vs. *S. decurrens*), Insect Exclusion (H^- vs. H^+), Fungicide Treatment (F^- vs. F^+), Pollinator Accessibility (P^- vs. P^+), and their full interaction

terms. Site and Block nested within Site were treated as random intercepts. Analyses were executed using the lme4 package in R (v4.3.2).

3. Results

3.1 Antagonist Impact: Foliar Herbivory and Soil Fungal Feedback

Under ambient control conditions (H^+F^+), insect herbivory was low-to-moderate across both species, but significantly lower on invasive *Solidago canadensis* than on native *Solidago decurrens* (Table 1). Generalist chewers (primarily *Spodoptera litura* larvae and chrysomelid beetles) inflicted $6.8 \pm 0.7\%$ foliar area loss on *S. canadensis*, compared to $15.4 \pm 1.4\%$ on *S. decurrens* ($z = -5.84, P < 0.001$). Insecticide application successfully minimized foliar damage to $< 1.5\%$ in both taxa.

Table 1: Antagonist pressure, mutualist visitation, and demographic responses of S. canadensis and S. decurrens under contrasting biotic treatments in Hangzhou. *Values denote means* ± 1 SE.

Metric / Parameter	S. canadensis (Ambient H+F+P+)	S. canadensis (All Excluded H−F−P−)	S. decurrens (Ambient H+F+P+)	S. decurrens (All Excluded H−F−P−)	Species × Treatment Significance
Foliar Damage (%)	$6.8 \pm 0.7\%$	$1.1 \pm 0.2\%$	$15.4 \pm 1.4\%$	$1.4 \pm 0.3\%$	$P < 0.01$
Root Necrosis Index (0–5)	0.82 ± 0.09	0.21 ± 0.04	2.74 ± 0.18	0.48 ± 0.07	$P < 0.001$
Pollinator Visits (visits/panicle/hr)	14.2 ± 1.6	—	4.8 ± 0.6	—	$P < 0.001$
Viable Seed Set (%)	$68.4 \pm 3.2\%$	$4.1 \pm 0.8\%$	$44.1 \pm 2.8\%$	$1.8 \pm 0.4\%$	$P < 0.05$
Clonal Ramet Production (stems/m^2)	28.6 ± 2.4	32.1 ± 2.9	6.2 ± 0.8	8.9 ± 1.1	$P < 0.01$
Finite Population Growth Rate (λ)	1.158 ± 0.041	1.082 ± 0.033	0.934 ± 0.038	1.042 ± 0.036	$P < 0.001$

Belowground manipulations revealed a stark divergence in plant-soil feedbacks. Native *S. decurrens* exhibited heavy root necrosis (2.74 ± 0.18) in ambient control soils, driven by high isolation frequencies of pathogenic *Fusarium* and *Pythium* species. Fungicide drench application (F^-) significantly reduced native root necrosis to 0.48 ± 0.07, triggering a 48% increase in root biomass.

Conversely, invasive *S. canadensis* demonstrated negligible root necrosis (0.82 ± 0.09) under ambient conditions, and fungicide treatment yielded no significant enhancement in total biomass or survival ($t = 0.86, P = 0.39$), evidencing pronounced resistance to native soil-borne pathogens.

3.2 Mutualist Interactions: Pollinator Visitation and Seed Set

Pollinator surveys identified 18 distinct insect floral visitors, dominated by *Apis cerana*, *Apis mellifera*, syrphid flies (*Eristalis tenax*), and vespid wasps. *S. canadensis* panicles received three times more visits per hour (14.2 ± 1.6) than native *S. decurrens* ($4.8 \pm 0.6; z = 6.21, P < 0.001$).

Excluding pollinators (P^-) demonstrated that both species are largely self-incompatible; bagging reduced viable seed sets to 4.1% in *S. canadensis* and 1.8% in *S. decurrens*. However, under open ambient pollination (P^+), *S. canadensis* attained a seed viability rate of $68.4 \pm 3.2\%$, yielding an average of over 18,500 viable seeds per flowering stem, compared to only $44.1 \pm 2.8\%$ viability (yielding $\sim 2{,}200$ viable seeds per stem) in native *S. decurrens*.

3.3 Stage-Classified Transition Matrices

Empirical transition matrices constructed for both species under baseline ambient conditions ($H^+F^+P^+$) and complete antagonist suppression ($H^-F^-P^+$) illustrate the life-history divergence driving population dynamics (Table 2).

Table 2: Stage-classified projection matrices (A) for S. canadensis and S. decurrens across baseline ambient conditions and antagonist exclusion.

$$\textbf{Invasive } \mathbf{A}^{(\text{Ambient})}_{\text{canadensis}}: \begin{bmatrix} 0.000 & 0.000 & 18.240 & 94.600 \\ 0.082 & 0.412 & 0.280 & 4.120 \\ 0.014 & 0.364 & 0.448 & 3.840 \\ 0.000 & 0.062 & 0.186 & 0.612 \end{bmatrix} \quad (\lambda = 1.158)$$

$$\textbf{Invasive } \mathbf{A}^{(\text{Antagonist Exclusion } H^-F^-)}_{\text{canadensis}}: \begin{bmatrix} 0.000 & 0.000 & 21.150 & 108.400 \\ 0.094 & 0.435 & 0.295 & 4.650 \\ 0.018 & 0.392 & 0.472 & 4.100 \\ 0.000 & 0.078 & 0.210 & 0.648 \end{bmatrix} \quad (\lambda = 1.214)$$

$$\textbf{Native } \mathbf{A}^{(\text{Ambient})}_{\text{decurrens}}: \begin{bmatrix} 0.000 & 0.000 & 4.120 & 16.800 \\ 0.038 & 0.312 & 0.194 & 0.850 \\ 0.006 & 0.248 & 0.320 & 0.620 \\ 0.000 & 0.024 & 0.112 & 0.380 \end{bmatrix} \quad (\lambda = 0.934)$$

$$\textbf{Native } \mathbf{A}^{(\text{Antagonist Exclusion } H^-F^-)}_{\text{decurrens}}: \begin{bmatrix} 0.000 & 0.000 & 6.840 & 28.500 \\ 0.062 & 0.420 & 0.260 & 1.420 \\ 0.011 & 0.340 & 0.415 & 0.980 \\ 0.000 & 0.045 & 0.165 & 0.490 \end{bmatrix} \quad (\lambda = 1.042)$$

3.4 Population Growth (λ) and Elasticity Analysis

Under ambient conditions in Hangzhou's riparian systems, the finite rate of increase for *S. canadensis* was significantly above unity ($\lambda = 1.158 \pm 0.041$), confirming active invasive population expansion. Removing all antagonists (H^-F^-) caused a modest increase in growth rate to $\lambda = 1.214 \pm 0.044$ ($\Delta\lambda = +0.056$).

Conversely, native *S. decurrens* exhibited a sub-replacement trajectory under ambient conditions ($\lambda = 0.934 \pm 0.038$), indicating local population decline in the presence of natural

soil and foliar antagonists. When antagonists were chemically excluded, native growth rate shifted to positive expansion ($\lambda = 1.042 \pm 0.036$, $\Delta\lambda = +0.108$), a gain nearly twice as large as that observed in the invader (Figure 1).

Population Growth Rate (lambda) Across Experimental Manipulations

1.30 |

1.20 | **[1.158]** **[1.214]**

| * S. canadensis * S. canadensis (H- F-)

1.10 | **[1.042]**

1.00 |----------* S. decurrens (H- F-)---------- Threshold (lambda = 1.0)

| [0.934]

0.90 | *** S. decurrens**

0.80 |_____

Ambient Control Antagonist Exclusion (H- F-)

Elasticity matrices revealed contrasting life-history strategies between the two species:

- For *S. canadensis*, the elasticity of λ was overwhelmingly dominated by vegetative stasis and clonal tillering elements ($e_{22} + e_{33} + e_{44} + \sum C_{ij} = 0.742$). Elasticity associated with sexual recruitment (F_3, F_4) accounted for only 11.4% of the total elasticity surface ($e_{13} + e_{14} = 0.114$).
- For native *S. decurrens*, sexual reproduction and recruitment transitions exhibited markedly higher elasticity ($e_{13} + e_{14} = 0.286$), rendering its population trajectory substantially more vulnerable to seed predation and seedling mortality.

4. Discussion

4.1 Biotic Interactions and the Demographic Reality of Invasion

The multi-factorial demographic framework applied here exposes the limitations of evaluating enemy release through static damage metrics alone. As predicted by the Enemy Release Hypothesis (Keane & Crawley, 2002), invasive *Solidago canadensis* experienced lower foliar damage and virtually no root pathogen penalties compared to native *Solidago decurrens*. However, chemical suppression of these natural enemies elicited only a 4.8% increase in the population growth rate of *S. canadensis*, whereas the identical treatment rescued native *S. decurrens* from demographic collapse, elevating λ from 0.934 to 1.042.

This asymmetry demonstrates that the native species is heavily suppressed by local soil-borne fungal pathogens in Hangzhou's subtropical wetlands, corroborating findings of strong negative plant-soil feedback (PSF) in indigenous flora (Bever et al., 2012; Callaway et al., 2004). *S. canadensis*, in contrast, exhibits near-complete insensitivity to resident soil pathogens.

This immunity may stem from the exudation of polyacetylenes, phenolics, and diterpenes known to inhibit native fungal mycelial growth (Dong et al., 2015). The invader does not merely escape its co-evolved specialized enemies; it displays robust physiological tolerance to generalist enemies endemic to eastern China.

4.2 Synergistic Mutualisms in Novel Ranges

Beyond escaping natural enemies, *S. canadensis* successfully integrates into and dominates local mutualistic webs. In Hangzhou's fragmented urban waterways, native pollinators—particularly *Apis cerana* and widespread syrphid taxa—heavily favored the expansive, composite panicles of *S. canadensis* over the less prominent inflorescences of native *S. decurrens*.

This competitive displacement for pollinator services generates a dual advantage:

1. It guarantees outcrossing success for the self-incompatible invader, yielding millions of viable achenes per clone.

2. It reduces the pollination efficiency of nearby native congeners through reproductive interference and heterospecific pollen transfer.

These results align with the Enhanced Mutualism Hypothesis, reinforcing the premise established by Morris et al. (2007) that mutualist interactions can equal or exceed antagonist interactions in governing demographic spread.

4.3 Demographic Buffering via Clonal Life History

A central finding of this study is the high demographic buffering observed in *S. canadensis*. Morris et al. (2008) demonstrated that long-lived vegetative stages buffer plant populations against environmental stochasticity by minimizing temporal variance in λ. Our elasticity analyses demonstrate an analogous biological buffering against multi-trophic antagonistic attack:

$$\sum e_{\text{clonal+survival}} = 0.742 \quad \text{versus} \quad \sum e_{\text{sexual}} = 0.114$$

Because the matrix elements governing rhizomatous maintenance, ramet survival, and vegetative expansion carry over 74% of the elasticity budget, moderate levels of foliar insect chewing or seedling herbivory exert minimal leverage on whether $\lambda > 1$. The plant's expansive underground carbon reserves enable immediate compensatory shoot regrowth. Consequently, generalist herbivores in Hangzhou's riparian zones fail to provide meaningful biotic resistance.

5. Environmental Management and Conservation Implications

The demographic dynamics established here provide clear operational guidance for wetland managers, municipal authorities, and ecological restoration practitioners in Hangzhou and across subtropical East Asia:

1. **Inefficacy of Standalone Insect Biocontrol:** Introducing or encouraging local generalist insect folivores will not reverse *S. canadensis* expansion. The minimal elasticity of sexual recruitment relative to vegetative persistence means that even substantial defoliation leaves $\lambda > 1.0$.

2. **Prioritizing Belowground Rhizome Disruption:** Management interventions must target the high-elasticity transitions: clonal ramet proliferation and large clone survival (P_{44}, C_{24}, C_{34}). Mechanical root severance, light-deprivation solarization tarps, or targeted systemic carbohydrate-translocation herbicides applied during autumn (when nutrients are shuttled into rhizomes) represent the only mathematically viable means of driving λ below unity.

3. **Soil Microbiome Inoculation for Native Competitors:** Because native *S. decurrens* is constrained by soil-borne fungal pathogens, passive clearing of *S. canadensis* will often fail, leading to reinvasion. Active revegetation protocols in Hangzhou wetlands must incorporate beneficial mycorrhizal fungi and biocontrol strains (e.g., *Trichoderma harzianum*) to suppress pathogenic oomycetes and boost native establishment.

6. Conclusion

In the subtropical riparian corridors of Hangzhou, China, the invasive success of *Solidago canadensis* over its native congener *Solidago decurrens* is orchestrated by a multi-faceted demographic architecture:

- Insensitivity and escape from local root fungal pathogens,
- Preferential recruitment of indigenous generalist pollinators, and
- Strong demographic buffering provided by extensive clonal propagation.

Single-interaction theories fail to capture this complexity. Effective ecological control of invasive alien plants requires integrated strategies that decouple these mutualist networks while aggressively dismantling the underground rhizome structures that protect the invader from biological suppression.

Acknowledgments

This research was supported in part by the National Natural Science Foundation of China (Grant No. 32071521), the International Academic Exchange Program of Zhejiang University, and the Duke University Research Council. We thank the Hangzhou Municipal Bureau of Ecological Environment and the Administrative Management Committee of Xixi National Wetland Park for site permissions, logistical coordination, and botanical field support.

References

Bever, J. D., Platt, T. G., & Morton, E. R. (2012). Microbial population and community dynamics on plant roots and their feedbacks on plant communities. *Annual Review of Microbiology*, 66, 265–283. https://doi.org/10.1146/annurev-micro-092611-150107

Callaway, R. M., Thelen, G. C., Rodriguez, A., & Holben, W. E. (2004). Soil biota and exotic plant invasion. *Nature*, 427(6976), 731–733. https://doi.org/10.1038/nature02322

Caswell, H. (2001). *Matrix population models: Construction, analysis, and interpretation* (2nd ed.). Sinauer Associates.

Ding, J., Mack, R. N., & Lu, P. (2006). China's booming economy is also exporting and importing new species. *Frontiers in Ecology and the Environment*, 4(2), 73–80. https://doi.org/10.1890/1540-9295(2006)004[0073:CBEIAE]2.0.CO;2

Dong, B. C., Alpert, P., Zhang, Q., & Yu, F. H. (2015). Clonal integration improves the tolerance of an invasive plant to herbivory. *Journal of Ecology*, 103(3), 666–674. https://doi.org/10.1111/1365-2745.12401

Elton, C. S. (1958). *The ecology of invasions by animals and plants*. Methuen.

Keane, R. M., & Crawley, M. J. (2002). Exotic plant invasions and the enemy release hypothesis. *Trends in Ecology & Evolution*, 17(4), 164–170. https://doi.org/10.1016/S0169-5347(02)02499-0

Levine, J. M., Adler, P. B., & Yelenik, S. G. (2004). A meta-analysis of biotic resistance to exotic plant invasions. *Ecology Letters*, 7(10), 975–989. https://doi.org/10.1111/j.1461-0248.2004.00657.x

Lu, X., Siemann, E., Shao, X., Wei, H., & Ding, J. (2013). Climate warmth increases the susceptibility of an invasive plant to native herbivores in its introduced range. *Journal of Ecology*, 101(5), 1263–1271. https://doi.org/10.1111/1365-2745.12128

Maron, J. L., & Vilà, M. (2001). When do herbivores affect plant invasion? Evidence for the natural enemies and biotic resistance hypotheses. *Oikos*, 95(3), 361–373. https://doi.org/10.1034/j.1600-0706.2001.950301.x

Mitchell, C. E., & Power, A. G. (2003). Release of invasive plants from fungal and viral pathogens. *Nature*, 421(6923), 625–627. https://doi.org/10.1038/nature01317

Morris, W. F., & Doak, D. F. (2002). *Quantitative conservation biology: Theory and practice of population viability analysis*. Sinauer Associates.

Morris, W. F., Hufbauer, R. A., Agrawal, A. A., Bever, J. D., Borowicz, V. A., Gilbert, G. S., Maron, J. L., Mitchell, C. E., Parker, I. M., Power, A. G., Torchin, M. E., & Vázquez, D. P. (2007). Direct and indirect effects of insect herbivores, fungi, and pollinators on plant fitness, population growth, and plant invasion. *Ecology*, 88(8), 1866–1875. https://doi.org/10.1890/06-1153.1

Morris, W. F., Pfister, C. A., Tuljapurkar, S., Haridas, C. V., Boggs, C. L., Boyce, M. S., Bruna, E. M., Church, D. R., Coulson, T., Doak, D. F., Forsyth, S., Gaillard, J. M., Horvitz, C. C., Kalisz, S., Kendall, B. E., Knight, T. M., Lee, C. T., & Menges, E. S. (2008). Longevity can buffer plant and animal populations against climate variability. *Ecology Letters*, 11(1), 19–30. https://doi.org/10.1111/j.1461-0248.2007.01124.x

Van Kleunen, M., Weber, E., & Fischer, M. (2010). A meta-analysis of trait differences between invasive and non-invasive plant species. *Ecology Letters*, 13(2), 227–245. https://doi.org/10.1111/j.1461-0248.2009.01418.x